Sansoni, Biancardi, Minoni & Docchio: A Novel, Adaptive System for 3-D Optical Profilometry Using a Liquid Crystal Light Projector

Thursday, February 11, 2021 2:01 PM

00310169

A Novel, Adaptive System for 3-D Optical Profilometry Using a Liquid Crystal Light Projector

Giovanna Sansoni, Luca Biancardi, Umberto Minoni, and Franco Docchio

***Abstract*— A 3-D optical whole-field profilometer based on adaptive projection of structured light is presented. The system is based on the projection of gratings by means of an LCD unit. The gratings can be varied both in contrast and in period, to adapt to the shape of the object under measurement. A video camera acquires at a different angle the object-deformed pattern. Suitable pre-elaboration is performed, to decrease dependence on background illumination and nonuniform reflectivity of the surface. Adaptive demodulation of the pattern allows the object profile to be evaluated.**

The performance of the instrument has been evaluated by means of a system calibration against a traceable high-precision commercial Contact Measuring Machine (CMM). The overall accuracy of the system is equal to 0.15 mm with a precision of 0.2 mm. In this article, the theoretical aspects of the technique are discussed, and the description of the complete system is presented. Profile reconstruction, calibration, and certification of the system are also covered. The accuracy of the system is discussed, and experimental results are presented.

I. Introduction

NONCONTACT, automatic optical instruments for topographic gauging are becoming increasingly relevant in the industrial environment for dimensional analysis and quality control [1]. These are, for example, 3-D contouring and gauging of large-surface car parts, or fast dimensional analysis of objects in relation to recognition of targets by robots [2]. Optical profilometry, in this context, plays a key role when applied to both macroscopic and microscopic measuring ranges.

Profilometry is generally implemented by using i) shading methods [3], ii) stereo vision methods, iii) single-spot laser scanners, or iv) structured light pattern projection [4]. In this last case, a structured light pattern is projected onto the object and reflected to a light sensor. The object topography is derived from the deformation of the light pattern, due to the shape of the object, by means of either direct analysis of the pattern or a suitable sampling mask (Moiré techniques) [5]–[7].

For all industrial applications, adaptiveness is a key requirement of profilometry. Adaptiveness, in fact, relates to the ability of the technique to modify the projection-detection combination according to the geometry of the particular target, and to the measuring parameters (distance, range, angle). Liquid crystal displays are suitable devices for adaptive projection [8]–[9]. They are robust and can be housed in projectors suitable for the industrial environment. On the other hand, adaptiveness has to be pursued with a proper design of the demodulation algorithm, which must be able to readily follow the changes in the projection pattern, also with reference to the target geometry.

We developed a whole-field profilometer based on structured light projection, with a high degree of flexibility. The description of the complete system shall be the subject of the present paper. In Section II, a brief outline of the technique shall be presented; Section III shall deal with the description of the hardware and software components of the system; Section IV shall present the main performances of the instrument, as it emerges from a set of experimental tests carried out on a prototype version of the system; finally, in Section V, both system calibration and certification are covered.

Manuscript received August 29, 1993. This work was supported in part by the European Community, Bureau of Community Reference, under Contract 3332/1/0/162/89/9-BCR-I(30).

The authors are with the Dipartimento di Elettronica per l'Automazione, Università degli Studi di Brescia, I-25123 Brescia, Italy.

IEEE Log Number 9402034.

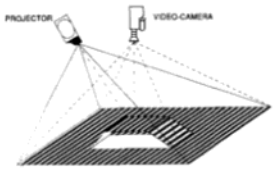

Fig. 1. Schematics of the approach to profilometry.

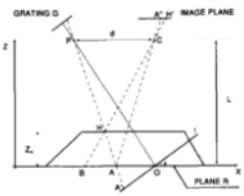

Fig. 2. Geometry of the projection and vision systems.

II. Overview of the Technique

Fig. 1 shows a schematic layout of the profilometer based on structured light illumination. The pattern (grating) projected onto the surface under measurement is observed at an angle: the resulting pattern, acquired by the video camera, is deformed according to the topography of the object. In order to extract the 3-D topographic information of the object, the 2-D deformed pattern is acquired by a video camera and then properly processed.

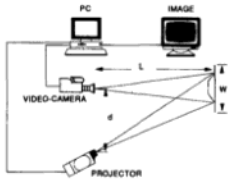

Fig. 3. Complete system layout of the profilometer.

A number of elaboration algorithms have been proposed [10]–[12]. The method adopted for our application is based on [12]. The basic outline of the technique is summarized with the aid of Fig. 2. The exit and entrance pupils of the projection and imaging optics are placed at points P and C, respectively; d is the distance between them and L the distance to reference plane R. Plane R coincides with the $x-y$ plane of the orthogonal coordinate system, and the z axis is parallel to the camera optical axis. The optical axes of both the projector and the camera intersect plane R at point O. The object height $Z(x,y)$ is evaluated with respect to plane R. G is a Ronchi grating, having its lines normal to the plane of the figure. Its image, on plane I, has a constant period p_0. When no object is placed on plane R, (i.e., $Z(x,y) \equiv 0$), the projected grating $G(x,y)$, observed on the image plane, presents a period $p(x)$ that increases with increasing x. $G(x,y)$ can be interpreted as a Fourier expansion of signals with spatial carrier frequencies $n/p = n\cos\vartheta/p_0$ modulated both in amplitude, given the nonuniform reflectivity of the surface of plane R, and in phase, given the variation of $p(x)$ along the x coordinate. In the presence of an object with a profile $Z(x,y)$, the grating observed at the image plane is further deformed. In fact, when $Z(x,y) = 0$, ray PA' strikes plane R at point A, which is imaged at point A'' in the image plane. In contrast, in the presence of an object, ray PA' strikes the object at point H, which is imaged onto point H' on the image plane. This means that, on plane R, point A moves to point B. Thus, the resulting grating $G_O(x,y)$ is phase-modulated by the variation of $p(x)$ along the x coordinate and by the lateral shift $\overline{BA}$ of ray PA', due to the presence of the object.

The height $Z_H(x,y)$ of the object at any point $H(x,y)$ can be evaluated by triangulation. Observing that triangles PHC and BHA are similar, we obtain

$$\frac{L - Z_H}{d} = \frac{Z_H}{\overline{BA}}. \tag{1}$$

Introducing the term $\Delta\Phi(x,y)$, i.e., the difference between the phases that modulate the grating in the presence and in the absence of the object, respectively, it can be demonstrated that

$$\Delta\Phi(x,y) = \frac{2\pi}{p}\overline{BA}. \tag{2}$$

Thus, calculation of the local height Z_H reduces to phase mapping of all points along the plane. Once the phase information $\Delta\Phi(x,y)$ is obtained, the object profile can be evaluated

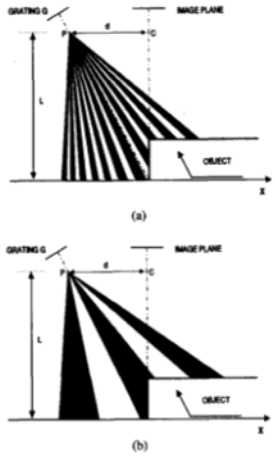

Fig. 4. Adaptation of the fringe spacing to the target topology. (a) Projection of a coarse grating. (b) Projection of a fine grating.

by the formula

$$Z(x,y) = Lp\Delta\Phi(x,y)/[2\pi d + p\Delta\Phi(x,y)]. \tag{3}$$

By applying a suitable demodulation procedure to both signals $G(x,y)$ and $G_O(x,y)$, the term $\Delta\Phi(x,y)$ can be evaluated. The adopted demodulation algorithm processes the deformed pattern in the real-signal domain by using demodulation and low-pass filtering procedures [12]. In our system, this procedure has been improved with respect to its original version, to enhance the adaptiveness features of the system and to reduce the computation time [13]. The main characteristics of the algorithm are: i) fast elaboration, to adapt to coarse changes of the grating period p, ii) the ability to tolerate fine variations of the grating period p, iii) the absence of strict requirements in the hardware architecture, iv) the ability to operate on an arbitrary number of pixels, and v) the need of only one image of the deformed pattern to perform the measurement.

III. System Description

A. System Layout

Fig. 3 shows the complete system layout of the profilometer. According to the projection geometry of Fig. 2, the centers of the pupils in the projection and imaging optics are located at the same distance L from the reference plane, and d is the distance between them. An LCD-based adaptive projection unit (LCD 320 ABW line projector) is used for the projection. This device is able to project gratings of variable period and contrast as well as a continuous gray code sequence. Through its built-in RS232 interface, the projector can be directly controlled by a personal computer (PC in the figure): this allows us to

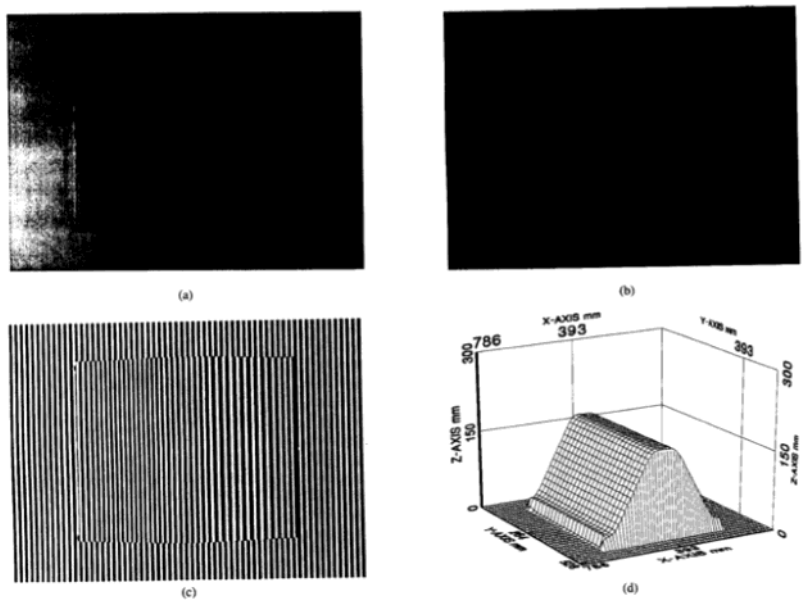

Fig. 5. Measurement performed on a uniformly reflective object. (a) Image of the object illuminated by the projector in the absence of the grating. (b) Image of the object illuminated by the projector in the presence of the grating. (c) Normalized image. (d) Plot of the calculated profile.

adapt the grating to both the shape of the object (by on-line modifying its period), and the background illumination l+evel (by varying its contrast). This projector produces flicker-free, long-term stable and high-contrast gratings.

The projected pattern is acquired by a black and white CCD video camera SONY XC-77CE, in the CCIR standard. The video camera can be equipped with both fixed optics (VCL-50Y-M, $f/2.8$) and CCTV precision zoom optics (Manual Iris 12.5–75 mm, $f/1.8$). It acquires images with a resolution equal to 512 × 512 pixels. The images are grabbed and stored by dedicated boards (Imaging Technology: AFG series), plugged into the PC (COMPAQ 386/E). The PC is equipped with dedicated libraries, to perform image acquisition and storage, and a wide range of image-processing operations, (pixel by pixel and area, and look-up table transformations). Image sampling is performed within the frame-time, i.e., at a frequency of 25 Hz. The frame memory is 1024 × 1024 pixels wide, and each pixel can be coded at 8, 12, and 16 bits. Consequently, up to 4 images of 512 × 512 pixels can be simultaneously stored and elaborated. The AFG boards are connected to a graphic monitor, to visualize the images stored in the frame memory. Actually, all the procedures needed to perform the measurement are coordinated by the software control unit implemented on the personal computer.

B. Software Environment

The control unit is based on a structure of nested menus. The first menu level is resident. Single items of this menu can be activated by the user. These can, in turn, activate nested menus or directly perform their tasks. The software has been developed in the C language.

The user interface allows the operator to directly i) drive the projector unit, ii) set the geometrical parameters of the system, iii) start the image acquisition, iv) perform the measurement, v) visualize the results of elaboration, and vi) calibrate the system. The interface provides the user with considerable flexibility in the choice of the procedures to be activated. Moreover, it handles user errors and incorrect parameter data entry. This feature becomes particularly important when the profilometer is envisaged to operate in industrial environments. As already mentioned, measurements are performed by activating suitable procedures in the proper sequence. In the following, the most significant among them are described.

C. System Procedures

Image Pre-elaboration: This procedure is automatically activated in parallel with image acquisition. Image acquisition consists of a sequence of steps. Three images of the object under measurement are acquired in the following illumina-

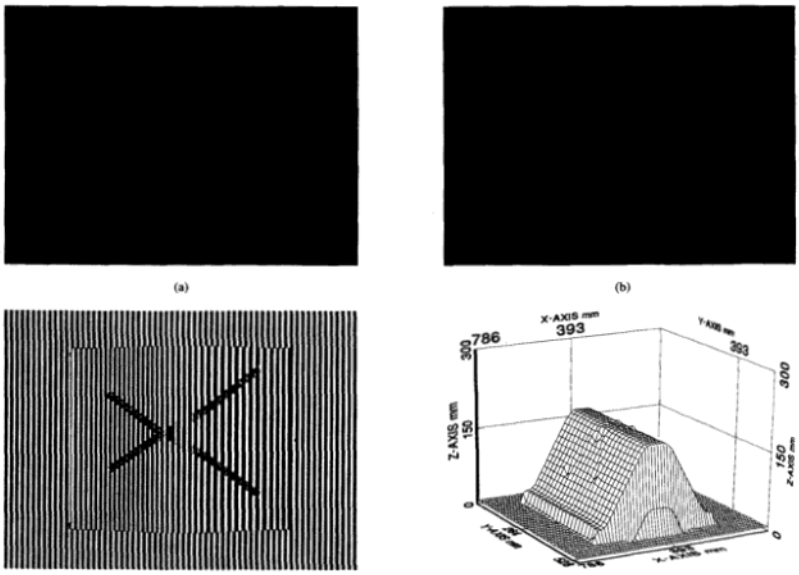

Fig. 6. Example of measurement in the case of highly varying properties of the surface. (a) Image of the object illuminated by the projector in the absence of the grating. (b) Image of the object illuminated by the projector in the presence of the grating. (c) Normalized image. (d) Plot of the calculated profile.

tion conditions: 1) environmental illumination, 2) projector illumination without grating, and 3) projector illumination with grating. Each of these images is averaged over a user-selectable number of frames. Starting from these images, gray-level normalization is performed according to the formula

$$i_{jk} = \frac{i^3_{jk} - i^1_{jk}}{i^2_{jk} - i^1_{jk}} \cdot NP \quad 1 \le j \le 512, 1 \le k \le 512. \qquad (4)$$

In this formula, $i^n_{jk}\,(n = 1, 2, 3)$ represents the gray level coded by the byte on the jth row and kth column of the matrix of 512×512 bytes associated to the image n. Images 1, 2, and 3 are those acquired in the three different illumination conditions, NP is a user-selectable parameter, which is required to set the gray-level dynamics, and i_{jk} is the intensity associated at each point of the normalized image.

The effect of the elaboration is to reduce the influence of background illumination and of nonuniformities of the object reflectivity on the resulting image, without losing the phase information related to the profile of the object. The algorithm is simple and effective and requires a short elaboration time. According to the procedure described so far, the projector is automatically switched on and off synchronously with image acquisition and averaging. The acquisition of the three averaged images takes about 12 s, while the elaboration takes place in 2 s. After this time the output image is available on the image monitor.

Profile Evaluation: The procedure that performs the profile evaluation is responsible for i) handling the geometrical parameters L and d of the system, ii) evaluating the carrier frequency of the grating on the reference plane, and iii) activating the demodulation algorithm to be applied on the normalized image. The first task is basically performed through a suitable data entry session. The second task automatically measures the grating period $p = p_0/\cos\vartheta$ which is an important parameter for the elaboration, according to (3). The last one is based on the algorithm described in Section II.

As already mentioned, the profile of the object is evaluated with respect to a reference surface (either real or virtual), over which the object is placed. Demodulation is applied to the image of the grating deformed by the reference plane, to obtain the so-called *reference phase map*. This phase map must be acquired once after setting up the profilometer, and whenever a profilometer calibration is needed. During profile gauging, the same elaboration procedure is applied to the normalized image of the grating deformed by the object under measurement, to obtain the so-called *object phase map*. The actual profile is then evaluated by applying (3) where $\Delta\Phi(x, y)$ is the difference between the two maps.

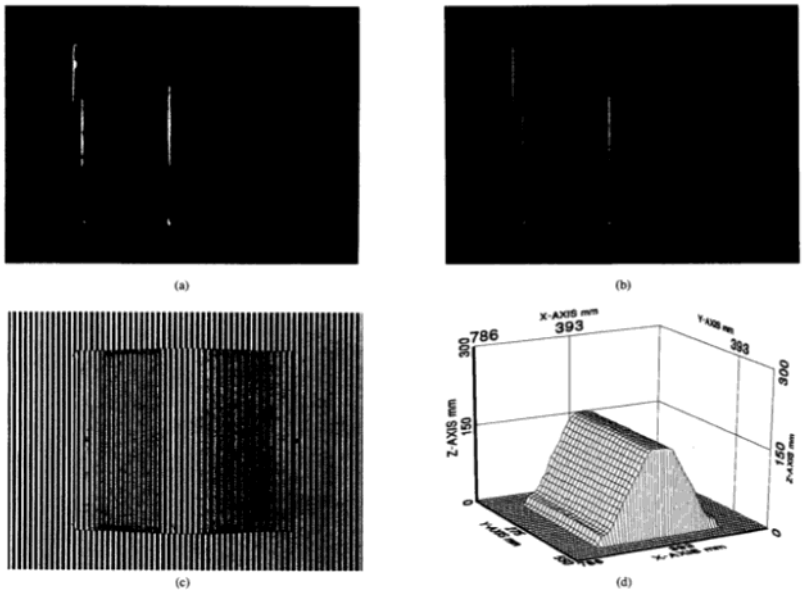

Fig. 7. Example of measurement on a reflective surface. (a) Image of the object illuminated by the projector in the absence of the grating. (b) Image of the object illuminated by the projector in the presence of the grating. (c) Normalized image. (d) Plot of the calculated profile.

In order to obtain the profile with correspondence of both coarse and fine surface variations, the capability of the system to adapt the fringe spacing to the target topology has been used. Fig. 4 schematically shows a typical situation. Figure 4(a) presents the projection of a coarse grating. In this situation, a half-period falls on the steep variation of the object, and no fringes are lost in the deformed grating acquired by the video camera. Correspondingly, the phase is evaluated without ambiguity: however, the resolution of the measurement, which depends on the grating period, is low. Thus, it is expected that the measured profile is not accurate in a relatively large region around the steep surface variation. Fig. 4(b) presents the projection of a fine grating. In this case, more than one period is projected on the region corresponding to the discontinuity of the surface. Consequently, an unknown number of fringes are lost in the deformed grating acquired by the video camera. Correspondingly, the phase is evaluated with an ambiguity. However, the resolution of the measurement is higher with respect to the previous case due to the finer period used in the demodulation.

In order to obtain a profile measured with the resolution given by the finer grating and the range given by the coarse grating, a suitable procedure has been developed, to match the information derived by the two different projection situations.

As a first step, the object is illuminated by a coarse grating, to perform the range measurement with correspondence of steep height variations. Secondly, a finer grating is projected, able to obtain a higher resolution of the profile measurement. The use of the LCD projector allows performance of these steps in a short time. The matching procedure combines the two measurements.

D. System Calibration

The calibration procedure allows the user to accurately determine the geometrical parameters of the system, as well as the demodulation parameters. An object with a known profile, namely the master, is used to calibrate the profilometer. The master has been characterized as described in Section V. After a coarse approximation of the profilometer parameters, the master is measured by the profilometer. Calibration is performed by evaluating the difference between the measured and the actual profile of the master. A calibration map is produced, where the height calculated by the profilometer and its error are presented for each calibration point. This procedure is repeated until the required measurement accuracy is obtained.

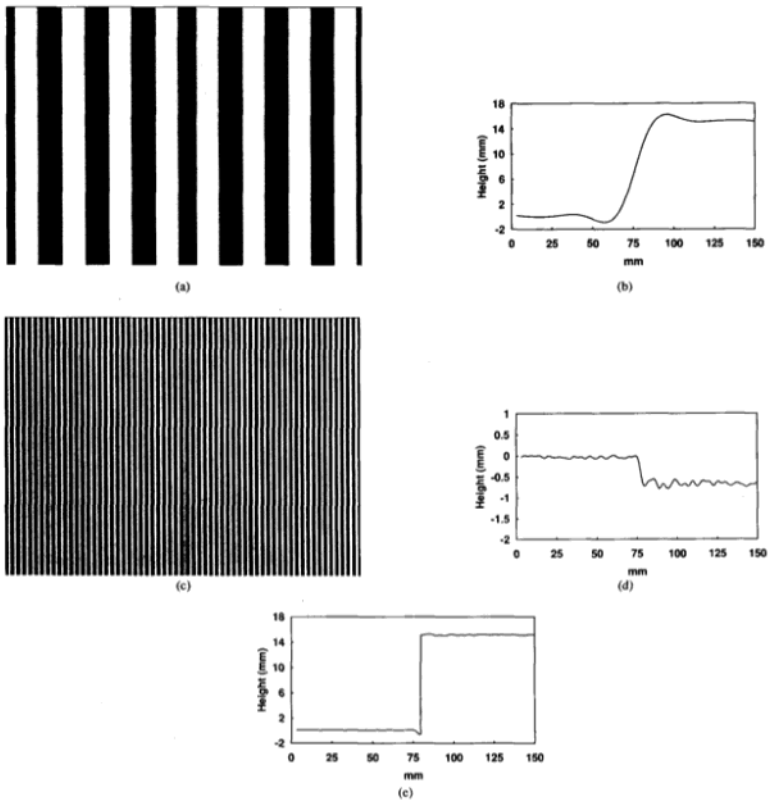

Fig. 8. Example of measurement performed by using two gratings with different period. (a) Normalized image of the object illuminated by a coarse grating (period 19.4 mm). (b) Evaluated profile. (c) Normalized image of the object illuminated by a fine grating (period 2.4 mm). (d) Evaluated profile. (e) Object profile obtained by combining the profiles previously obtained.

IV. Experimental Results

A. Evaluation of System Performance

Experiments aimed at evaluating the system performance have been made using various objects. A first, interesting result concerns the profile measurement of the object shown in Fig. 5(a). The geometric system parameters L and d are equal to 5 m and 1 m, respectively, and the illuminated field is equal to 786 × 528 mm. The mean period of the grating on the reference plane is equal to 12.5 mm. The object presents a trapezoidal shape. In this case, the object is light gray-painted, and the surface appears uniformly diffusive. Fig. 5(b) shows the object illuminated by the projector in the presence of fringes. The deformed pattern after the normalization procedure is presented in Fig. 5(c), and the profile of the object is plotted in Fig. 5(d).

In order to test the system performance in the case of highly varying properties of the surface, we placed two black stripes on the object of Fig. 5. Figs. 6(a) and (b) show the object illuminated by the projector in the absence and in the presence of the grating, respectively. The normalized image is shown in Fig. 6(c). Note that, in the central, flat region of the object, the fringes are perfectly reconstructed. With correspondence of the object sides, despite the fact that light is reflected in a different direction with respect to that of the video camera, the fringes are significantly well reconstructed. Fig. 6(d) shows the calculated profile.

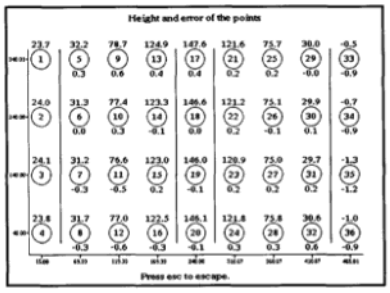

Fig. 9. Calibration map of the selected points used to calibrate the profilometer.

An example of a measurement performed on a reflective surface is presented in Fig. 7. The geometric system parameters are the same as in the example of Fig. 5. Figs. 7(a) and (b) show the surface illuminated by the projector in the absence and in the presence of the grating. Again, normalization allows us to precisely reconstruct the deformed pattern [see Fig. 7(c)], and the object profile of Fig. 7(d) has been evaluated.

B. Adaptiveness Evaluation

The advantages of the capability of the system to adapt the fringe spacing to the target topology have been verified on a set of experiments. As a typical result, the profile measurement of an object presenting a steep height variation is shown in Fig. 8. The object has a parallelepiped shape of dimensions $15 \times 150 \times 130$ mm $(h \times w \times l)$. In the experiment, the geometry of Fig. 4 has been chosen, where the geometric parameters of the system are $L = 1$ m and $d = 150$ mm. The field of view is equal to 150×106 mm.

A coarse grating has been projected on the object. Fig. 8(a) presents the resulting normalized image. The mean period of the undeformed grating was 19.4 mm. Note the central black fringe of the grating, deformed by the height variation of the object. The profile measurement of a section of the object along the x-coordinate is shown in Fig. 8(b). The plot represents the profile corresponding to row no. 255 of the image. It can be noted that i) the projection of the coarse period allows us to perform the range measurement, and ii) the profile of the object is not well reconstructed around the steep height variation, as expected. This region is estimated to be 80 mm wide, corresponding to about four times the projected period. In order to increase the measurement resolution, a finer grating has been projected on the object. Fig. 8(c) presents the corresponding normalized image. The mean period of the undeformed grating was 2.4 mm. The profile measurement along the same section of the object is shown in Fig. 8(d). Now the steep height variation is lost. Correspondingly, the phase is evaluated with an ambiguity. However, the profile of the flat regions before and after the discontinuity is evaluated with a resolution higher with respect to the previous case.

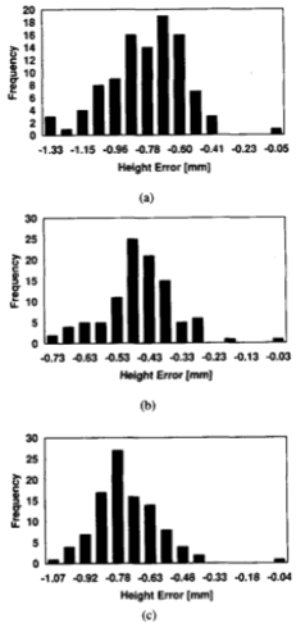

Fig. 10. Height error distribution of the set of measurements of three out of thirty-six points used for calibration. (a) Error distribution of the measurements of point 8. (b) Error distribution of the measurements of point 17. (c) Error distribution of the measurements of point 18.

Again, the ambiguity region is four times the projected period. In this case, it is equal to 10 mm. In order to obtain the profile with correspondence of both fine and coarse variations, the information obtained so far has been combined. The resulting profile is shown in Fig. 8(e).

V. Calibration and Certification

A master object has been used for the calibration of the whole-field profilometer. The object is the same as shown in Fig. 4(a). Thirty-six points have been selected on its surface. A coordinate system has been set on the object. It has been used to evaluate both the measurements performed by a Contact Measurement Machine (CMM) and those resulting from the whole-field profilometer. The geometric system parameters were the same as in the example of Fig. 5. The measurements obtained from both the CMM and the optical profilometer have been compared by using the calibration procedure. The procedure has been iterated until the errors became less than 1 mm. As a result of the elaboration, the map of Fig. 9 has been obtained. This map presents, for each point, the height calculated by the profilometer (above the circle) and the error

with respect to the measurement done by the CMM system (below the circle). The measurement unit is the millimeter. Points labeled from 1 to 4 have been used as a reference to evaluate the height of the other points. For example, the height of the points labeled from 5 to 33 is evaluated as the difference between the height of each point and the height of the point labeled 1.

In order to certify the whole-field profilometer, ten groups of measurements have been made. Each group includes one measurement of the reference plane and ten measurements of the master profile. The total amount of images elaborated is equal to 110. This procedure has been repeated with different contrasts of the projected gratings. The profilometer parameters were the same ones used for calibration. For each image, a calibration map has been produced, and, for each point of the map, both the mean value and the mean square error have been calculated on the set of 100 measurements.

A statistical analysis of the measurement errors has been performed. In the case of maximum contrast of the gratings, the system accuracy is equal to 0.158 mm with a precision of 0.2 mm. In the case of half contrast, the system accuracy is equal to 0.218 mm, with a precision equal to 0.217 mm. The distribution of the height errors related to each measurement point has been evaluated to be close to a Gaussian distribution. Fig. 10 shows three examples, related to points 8, 17, and 18, respectively.

VI. Conclusion

A whole-field profilometer based on structured light projection has been presented here. An LC device is used as a projector, which provides the system with a high degree of flexibility. In fact, adaptiveness of the projection allows adaptation of the grating period to the shape of the object under measurement. Moreover, the possibility of synchronizing the grating projection with the image acquisition leads to a fast implementation of suitable image normalization procedures, and this results in a low dependence of the measurement accuracy on background illumination as well as on nonuniformities of the object surface. The adopted demodulation algorithm leads to accurate phase evaluation, resulting in good accuracy of the measured profiles.

Acknowledgment

The authors are indebted to Prof. A. Taroni for useful suggestions in the preparation of this manuscript.

References

[1] D. Poussart and D. Laurendeau, "3-D sensing for industrial computer vision," in *Advances in Machine Vision*, J. L. C. Sanz, Ed. New York: Springer-Verlag, 1989.
[2] K. G. Wesolowicz and R. E. Sampson, "3-D imaging sensor for robotic applications," in *Conf. Rec. 5th ICALEO*, IFS Publications, 1987.
[3] B. K. P. Horn, "The variational approach to shape from shading," MIT AI Memo 813, 1985.
[4] G. Sansoni, F. Docchio, U. Minoni, and L. Biancardi, "Adaptive profilometry for industrial applications," in *Laser Applications to Mechanical Industry*, S. Martellucci and A. N. Chester Eds. Norwell, MA: Kluwer Academic, 1993, pp. 351–365.
[5] M. Idesawa, T. Yatagui, and T. Soma, "Scanning Moiré method and automatic measurement of 3-D shapes," *Appl. Opt.*, vol. 16, pp. 2152–2162, 1977.
[6] D. T. Moore and B. E. Truax, "Phase-locked Moiré fringe analysis for automated contouring of diffuse surfaces," *Appl. Opt.*, vol. 18, pp. 91–96, 1979.
[7] G. Indebetouw, "Profile measurement using projection of running fringes," *Appl. Opt.*, vol. 17, pp. 2930–2933, 1978.
[8] G. Sansoni, F. Docchio, U. Minoni, and N. Viviani, "Characterization of commercial liquid crystal displays for adaptive pattern projection in industrial profilometry," *Int. J. Optoelectron.*, vol. 8, pp. 685–704, 1993.
[9] F. Docchio, G. Sansoni, U. Minoni, and N. Viviani, "Light-induced transmission changes in liquid crystal displays for adaptive pattern projection," *IEEE Trans. Instrum. Meas.*, vol. 41, pp. 629–632, 1992.
[10] M. Takeda and K. Mutoh, "Fourier transform profilometry for the automatic measurement of 3-D object shapes," *Appl. Opt.*, vol. 22, pp. 3977–3982, 1983.
[11] V. Srinivasan, H. C. Liu, and M. Halioua, "Automated phase-measuring profilometry: A phase mapping approach," *Appl. Opt.*, vol. 24, pp. 185–188, 1985.
[12] S. Tang and Y.Y Hung, "Fast profilometer for the automatic measurement of 3-D object shapes," *Appl. Opt.*, vol. 29, pp. 3012–3018, 1990.
[13] G. Sansoni, L. Biancardi, F. Docchio, and U. Minoni, "Comparative analysis of low-pass filters for the demodulation of projected gratings in 3-D adaptive profilometry," *IEEE Trans. Instrum. Meas.*, vol. 43, pp. 50–55, 1994.

Giovanna Sansoni received the degree in electronic engineering from the Politecnico of Milan, Italy, in 1984.

In 1985 she joined the Dipartimento di Automazione Industriale (now Dipartimento di Elettronica per l'Automazione) at the University of Brescia, Italy. Since 1986 she has been working as researcher and Assistant Professor in Electronic Instrumentation. Till 1989 her research interest was in the areas of computer-based instrumentation with emphasis on reliability and redundancy aspects, architectural aspects, and modeling techniques. The present involvement of her research activity is related to the characterization and the development of devices for image projection and elaboration with particular attention to the industrial application of such devices in noncontact optical profilometry.

Luca Biancardi was born in Mantova, Italy, in 1965. He received the degree in electronic engineering from the Politecnico of Milan, Italy, in 1989.

He has been working at the University of Brescia, at the Dipartimento of Scienze Biomediche e Biotecnologie, as research associate and at the Dipartimento di Elettronica per l'Automazione as research fellow in optoelectronics. He has been biomedical adviser for the Institute of Internal Medicine at the Spedali Civili di Brescia, Italy. His research activity is concentrated in the areas of digital signal processing and image processing, with particular reference to the development, characterization, and test of electrooptical instrumentation for industrial metrology.

Umberto Minoni was born in 1960. He received the M.S. degree in mechanical engineering from the University of Brescia in 1984.

He joined the Dipartimento di Automazione Industriale (now Dipartimento di Elettronica per l'Automazione) at the University of Brescia where he presently is a Researcher and Assistant Professor in Electronic Instrumentation. His research activities cover the field of industrial measurements for automated production systems. The main research activities are related to the application of optical techniques for dimensional gauging and for the development of new measurement systems for industrial applications.

Franco Docchio received the degree in nuclear engineering from the Politecnico of Milan, Italy, in 1976.

He joined the Centro di Elettronica Quantistica of the National Research Council of Italy in 1978, where he carried out research concerning laser development, laser applications in industry and bio-medicine, development of microprocessor-based instrumentation, and laser-tissue interaction. In 1987 he joined the Dipartimento di Automazione Industriale (now Dipartimento di Elettronica per l'Automazione) at the University of Brescia, where he presently holds the Associate Professorship of Optoelectronics. The present involvement of his research group ranges from the development of novel electrooptical instrumentation for industrial metrology and calibration, to the investigation of devices for image projection and elaboration, and to the measurement and compensation of robot positioning errors.

Dr. Docchio is the author of more than 120 research papers. He is a member of SPIE, of the European Society for Engineering and Medicine, of the Italian Society for Optics and Photonics, of the Italian Society for Lasers in Ophthalmology, and is part of the Management Committee for the European Concerted Action on Ocular Fluorometry.